Observation of Supercurrent Drag between Normal Metal and Superconducting Films

Xiaokang Huang, Greg Bazàn, and Gary H. Bernstein*
Department of Electrical Engineering, University of Notre Dame, Notre Dame, Indiana 46556
(Received 1 September 1994)

We experimentally investigate the Coulomb interaction between normal metal (Au/Ti) and superconducting (AlO_x) 2D films separated by an insulating (Al_2O_3) layer. We report here the observation of supercurrent drag predicted by Duan and Yip [Phys. Rev. Lett. **70**, 3647 (1993)]. The drag was observed at temperatures close to T_c, with the ratio of the drag current to the drive current as high as about 1×10^{-3}. Our results are discussed in terms of a model of Coulomb mutual scattering between the normal electrons in the drive wire and the superelectrons in the drag wire.

PACS numbers: 73.20.Dx, 73.50.–h, 73.61.–r, 74.90.+n

Coulomb mutual scattering (CMS) between two proximate electron gases was first discussed theoretically by Price [1]. It was predicted that electrons in the two closely separated electron gases could exchange their momentum and energy via their Coulomb interaction, resulting in current drag. Coulomb drag was later experimentally observed between a two-dimensional electron gas (2DEG) and a three-dimensional electron gas (3DEG) [2], and also between two 2DEG's [3,4]. The samples in those experiments were GaAs/AlGaAs heterostructures. Although the CMS model can be used to qualitatively explain their results, some subtle effects, such as Peltier heating [2,4,5] and virtual phonon exchange [3,6], were also involved as secondary coupling mechanisms. Current drag in a magnetic field [7] and from the van der Waals interaction [8] was also investigated theoretically. CMS has not been experimentally observed in normal metal systems because of screening and dissipation.

Recently, Duan and Yip [9] theoretically studied the Coulomb interaction between two spatially separated superconducting systems that can be either two-dimensional (2D) films or one-dimensional (1D) lines. They concluded that a relatively strong supercurrent drag could result from the Coulomb interaction, with an estimated current drag-to-drive ratio between two 1D loops separated by 100 nm as high as 10^{-3}. This could also be true with normal metal as the input and the superconductor as the sensor [9]. The first experimental study on current coupling in a superconductor–normal metal system was recently reported by Giordano and Monnier [10]. However, the weak coupling and the similarity of their results to the behavior of vortices in high-T_c superconductors [11] led them to consider a mechanism of coupling other than supercurrent drag.

In this Letter, we report experimental results of the observation of supercurrent drag between a normal metal (Au/Ti) film and a superconducting (AlO_x) film separated by an insulator. Although a structure similar to that of Ref. [10] was used in our experiments, our samples were more than a hundred times smaller. Very strong current coupling ($\sim 10^{-3}$) was observed when the drive current was injected into the normal metal film and the open circuit voltage was detected at the superconducting side. There was no detectable coupling measured at the normal metal wire when the drive current was injected into the superconducting wire. The current coupling ratio as a function of temperature was fitted by a model of Coulomb mutual scattering between the electrons in the drive (normal metal) wire and the superelectrons in the drag (superconducting) wire.

A schematic diagram of the trilayer samples used in our current drag experiments is shown in Fig. 1. The bottom layer is 12/3 nm thick Au/Ti. Ti was used for adhesion between the Au layer and the SiO_2/Si substrate. The top layer is 30 nm thick AlO_x formed by bleeding O_2 with a pressure of 5×10^{-6} torr [12] into the vacuum chamber during Al evaporation. We chose AlO_x over pure Al in order to achieve a wide transition temperature region. This helped us to more accurately investigate the change of the current drag over the transition from the normal state to the superconducting state. The sheet resistance of the Au/Ti film was 8 Ω at room temperature. The sheet resistance of the AlO_x film ranged from 10 Ω to 2 kΩ at room temperature, depending on the percentage of O_2 in the Al film. An Al_2O_3 insulating layer, deposited by the same method as the AlO_x layer except with higher O_2 pressure (5×10^{-4} torr), was formed between the Au/Ti and the AlO_x. The relative dielectric constant of the Al_2O_3 was 4.5–6 as obtained by capacitance measurement, the breakdown voltage was 10^7 V/cm, and the thickness was 35 nm, as measured with a sur-

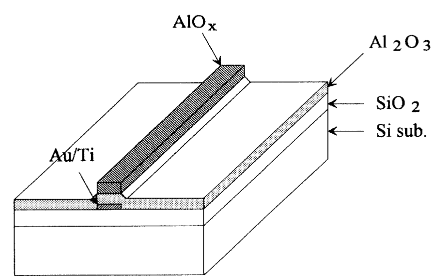

FIG. 1. Schematic of our device structure. The thickness of the Al_2O_3 separation was 35 nm and the overlapping area of the AlO_x and Au/Ti was 1×50 μm^2.

0031-9007/95/74(20)/4051(4)$06.00

face profiler. The thickness of our insulating layer prevented tunneling between the two conductive layers, resulting in a total leakage resistance between the two layers of $10^9 - 10^{12}\ \Omega$. Both the Au/Ti and AlO_x layers were 1 μm wide. Electron beam lithography was used to pattern the Au/Ti and the AlO_x in order to make the two layers totally overlap. The alignment error was $< \pm 0.05\ \mu$m [13] over an active area of $1 \times 50\ \mu m^2$. A 15 Hz ac current signal was sent into the primary (drive) side. The coupling signal at the secondary (drag) side was detected with a lock-in amplifier as an open circuit voltage.

It would be preferable to measure the short circuit drag current instead of the open circuit voltage from the secondary side. It is difficult to measure the current directly with a lock-in amplifier because the resistance of metal lines is very small at lower temperatures, and changes continuously over the transition region, becoming so small that it cannot drive the ammeter. This is because the low metal resistance, i.e., the source resistance of the drag wire as current source, short circuits the drag current from the ammeter. Therefore, we determined the supercurrent drag by measuring the open circuit voltage at the secondary side with a high impedance lock-in amplifier. As shown in Fig. 2(a), an input current I_1 is injected into the primary side. The electrons in the primary wire transfer their momentum to the electrons in the secondary wire via CMS [1], resulting in a drag current I_{drag} flowing in the same direction as I_1 and causing an accumulation of electrons at one end of the secondary wire, inducing an open circuit voltage V_{oc} at the secondary side. This induced voltage causes electrons to drift in the opposite direction within the wire, canceling the effects of drag ad resulting in net zero current. As shown in Fig. 2(a), the polarity of V_{oc} is opposite to that induced in the input loop by the input current I_1.

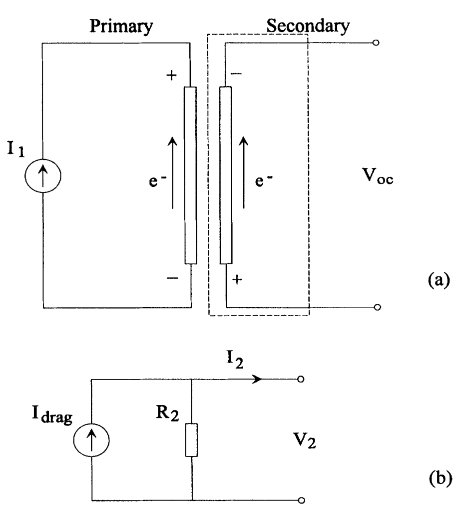

FIG. 2. (a) Circuit schematic of our test circuit. I_1 is the input current and V_{oc} is the measured open circuit voltage. (b) The equivalent circuit of the secondary wire. R_2 is the temperature dependent resistance of the secondary wire.

The equivalent circuit [14] of the secondary wire is shown in Fig. 2(b). The induced current I_{drag} is symbolized as a current source. R_2 is the resistance of the secondary wire. For short circuit conditions, $V_2 = 0$, which gives $I_2 = I_{sc} = I_{drag}$, while with the output loop open circuited, I_2 is zero. For open circuit conditions,

$$V_2 = V_{oc} = I_{drag} R_2 \quad \text{or} \quad I_{drag} = V_{oc}/R_2 . \qquad (1)$$

This simple relationship is very important since it shows that V_{oc} can give us a measure of I_{drag} provided that R_2 is known.

The resistance of the AlO_x film (sample 2a.1), R_2, was measured using a standard four-probe measurement with 5 nA input current. The change of the resistance as a function of temperature, ranging from 1.87 to 2.3 K, is shown in Fig. 3(a). It shows that the transition between the normal state and the superconducting state occurred in the temperature range from 1.93 to 2.05 K.

Figure 3(b) shows V_{oc} and V_{oc}/I_1 as a function of temperature. V_{oc} was measured at the AlO_x side when introducing the input current I_1 at the Au/Ti side. Several samples with the same size, but with different transition tem-

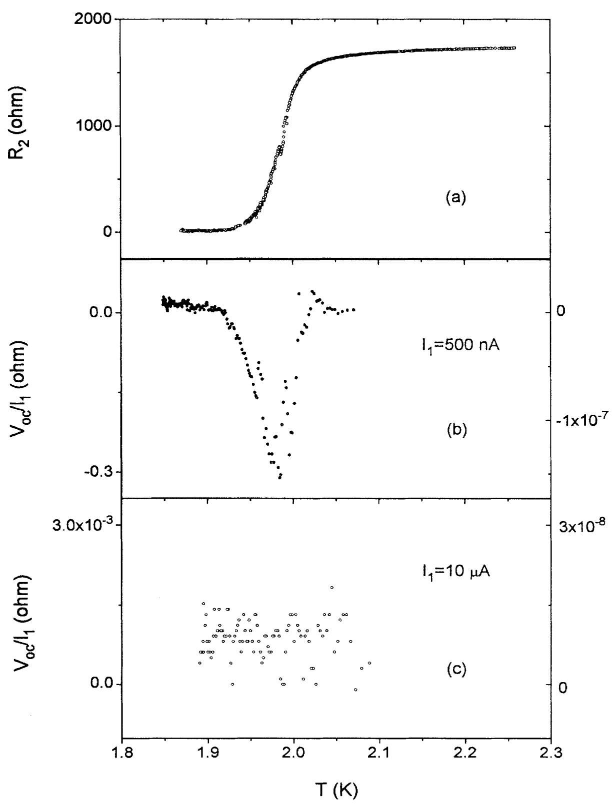

FIG. 3. (a) Temperature dependence of the resistance of the AlO_x. The transition temperature region was 1.93 to 2.05 K. (b) The ratio of the open circuit voltage, V_{oc}, to the input current I_1 as a function of temperature for I_1 injected into the Au/Ti wire and V_{oc} detected at the AlO_x. For convenience, data are also plotted as V_{oc}. (c) V_{oc}/I_1 as a function of temperature with I_1 injected into the AlO_x and V_{oc} measured at the Au/Ti.

peratures, were measured and the results were repeatable. Similar effects were also observed with a sample that consisted of 10 μm wide AlO_x and 20 μm wide Au/Ti layers separated by a 35 nm thick Al_2O_3 layer, although the coupling signal was more than 100 times weaker in this case.

As discussed above, V_{oc} (V_{oc}/I_1) is a function of both R_2 and I_{drag}, which are both temperature dependent. Comparing Figs. 3(a) and 3(b), we can see that when the temperature T is higher than the critical temperature of the AlO_x, there is no induced voltage detected. Since $V_{oc} = I_{drag}R_2$ and $R_2 \neq 0$, zero open circuit voltage means that there is no coupling current at this temperature range. The absence of coupling is due to the fact that the AlO_x is still in the normal state within this high-temperature region where the screening effect is strong and the normal electrons are dissipative. This also confirms that there is no detectable current coupling between two normal metal films for a barrier of 35 nm.

When the AlO_x starts to became superconducting at T below $\sim$2.0 K, some electrons form Cooper pairs and some are still in the normal state. Since Cooper pairs move freely without dissipation and interact within a coherence length that is much larger than the screening length in the normal state, a supercurrent I_{drag} results from the Coulomb interaction between the normal electrons in the drive line and the superelectrons in the drag line. Therefore, an open circuit voltage across the AlO_x line appears because $I_{drag} \neq 0$ and $R_2 \neq 0$ on this region. The magnitude of the induced voltage increases as temperature decreases and more electrons pair. This means that with decreasing temperature, although the resistance of the AlO_x decreases, the increase in the coupling current from the Coulomb interaction is much faster than is the decrease of the resistance.

The negative sign of V_{oc} means that its polarity is in the opposite direction relative to I_1, as discussed above. This indicates that the coupling current is in the same direction as I_1, which was expected [2–5,9] for a Coulomb interaction with momentum transfer between the electrons in the Au/Ti and Cooper pairs in the AlO_x. As the temperature decreases, the magnitude of V_{oc} reaches a maximum value when the increase of I_{drag} balances the decrease of R_2. After this, the magnitude of V_{oc} starts to drop toward zero with the temperature far below T_c because R_2 approaches zero in Eq. (1). The negative sign of V_{oc} also tells us that the induced voltage was not from leakage or tunneling, since in both cases the voltage in the drag line would be in the same direction as that in the drive line. As a further check, we measured the leakage current with 0.5 V bias applied between the two films and found the leakage resistance to be greater than 10^9 Ω with very little variation over the temperature range of interest. V_{oc} could be due to neither classical capacitive nor inductive coupling since either coupling would correspond to a nonzero voltage $\pm 90°$ out of phase relative to the input signal. We therefore measured the quadrature component simultaneously and found it to be much smaller than the in-phase component, with almost no variation over the temperature range and for frequencies from 15 to 1500 Hz.

The open circuit voltage was also measured at the Au/Ti film when AlO_x wire was used as the input. V_{oc}/I_1 for this case is shown in Fig. 3(c). It is important to note that the vertical scale of Fig. 3(c) is 10^2 times smaller than that of Fig. 3(b). From this figure, it is clear that no current coupling could be detected. Therefore, the current coupling from the superconducting wire to the normal metal wire was at least 10^3 times smaller than that of the reverse case. This asymmetric behavior of the current coupling provides more evidence that the detected current coupling was neither from electromagnetic coupling nor from quantum tunneling between the two films. Our data are in good agreement with supercurrent drag theory [9], as will be discussed further below. Since there was no coupling when the normal metal acted as the secondary wire, the current coupling and the coupling ratio mentioned below refer only to the case in which the Al/Ti is the primary wire and the AlO_x is the secondary wire.

The equivalent resistance V_{oc}/I_1, as a function of the input current I_1, was also investigated. As I_1 changed from 0.5 to 10 μA, the peak magnitude of V_{oc}/I_1 only fluctuated within $\pm 10\%$ of the peak value. However, the peak position moved toward lower temperatures with $I_1 > 2.5$ μA. This is possibly due to self-heating of the sample for large input current.

The temperature dependence discussed above is qualitatively similar to that reported in Ref. [10], but with much greater measured output voltages. The differences in sign and magnitude between our results and those of Ref. [10] imply that different mechanisms are involved in the two current coupling processes. CMS was ruled out in Ref. [10], whereas below we justify our interpretation in terms of CMS.

From Eq. (1), I_{drag} was calculated from V_{oc} and R_2 measurements, and is shown in Fig. 4(a) as the current coupling ratio I_{drag}/I_1. As expected, there was no current coupling when the AlO_x was in the normal state. At temperatures below T_c, I_{drag}/I_1 increased rapidly to values as high as about 1×10^{-3}. It is not surprising that the error of I_{drag}/I_1 increased as temperature decreased, since $I_{drag} = V_{oc}/R_2$. The absolute error of the drag current, δI_{drag}, can be written as

$$\delta I_{drag} = \pm\sqrt{(\delta V_{oc}/R_2)^2 + (V_{oc}\delta R_2/R_2^2)^2}, \qquad (2)$$

where δV_{oc} and δR_2 are the absolute errors of V_{oc} and R_2, respectively. Thus, when R_2 approaches zero, δI_{drag} approaches infinity. Therefore, V_{oc}/R_2 was used for calculating I_{drag} in Fig. 4(a) only when R_2 and V_{oc} were not too small, i.e., for temperatures close to T_c.

With reference to the Drude transport model, the drag current in the secondary wire can be considered part of the current flowing in the first wire but with a different scattering time, so the relationship between the coupling current and the mutual scattering rate can be expressed as

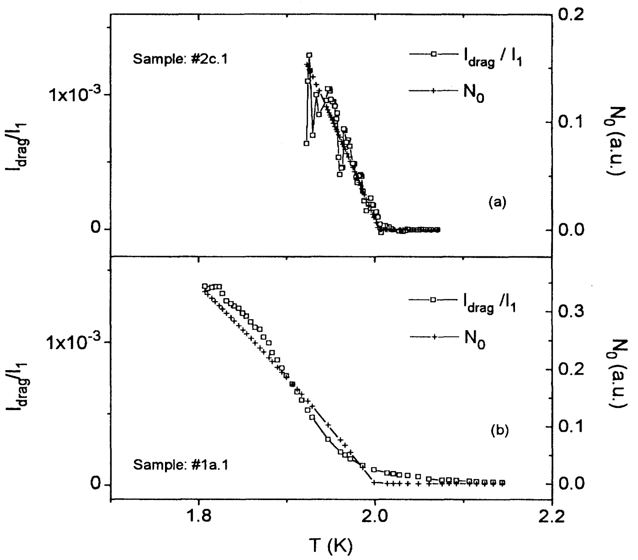

FIG. 4. The relationship between the current coupling ratio, $I_{\rm drag}/I_1 = V_{\rm oc}/R_2 I_1$, and temperature for sample 2c.1 (a) and 1a.1 (b). The normalized Cooper pair density as a function of temperature is also shown in the figures for comparison with the supercurrent drag theory.

$$I_{\rm drag} = (\tau_1/\tau_{12}) I_1 , \quad (3)$$

where τ_1 is the electron scattering time in the drive wire, and τ_{12} is the mutual scattering time between the two wires. The scattering rate $1/\tau_{12}$ is proportional to $N_1 N_2$ [1], that is,

$$1/\tau_{12} = K_{12} N_1 N_2 , \quad (4)$$

where K_{12} is a temperature independent coefficient. N_1 and N_2 are the electron and Cooper pair concentrations in the drive (normal metal) wire and the drag (superconducting) wire, respectively. Since N_1 is constant in the temperature region concerned, $1/\tau_{12}$ has the same temperature dependence as that of N_2. From $N_2 = N[1 - (T/T_c)^4]/2$ [15], where N is the total electron concentration in the superconducting wire, we have

$$I_{\rm drag}/I_1 \propto 1/\tau_{12} \propto N_2 \propto 1 - (T/T_c)^4 . \quad (5)$$

In Fig. 4(a) we also plot the normalized electron concentration $N_0 = 2N_2/N = 1 - (T/T_c)^4$ for T_c chosen as 2.005 K. The similarity between the shapes of $I_{\rm drag}/I_1$ and N_0 is strong evidence that the drag phenomenon is related to the pairing of electrons in the superconducting drag wire below the transition temperature.

Figure 4(b) shows $I_{\rm drag}/I_1$ and N_0 as a function of temperature from sample 1a.1. Although this sample was with the same geometry as 2c.1, its transition region was much larger due to its large sheet resistance (2 kΩ) of AlO_x wire. At our lowest temperature (1.8 K), the resistance was still larger than 15% of the resistance at 4.2 K. However, the detected $I_{\rm drag}/I_1$ had the same trend as N_0, as we saw in Fig. 4(a).

In conclusion, we believe that the observed current drag is due to phenomena predicted in Ref. [9], namely, supercurrent drag between normal electrons and Cooper pairs. First, this current coupling appeared only below T_c, and is therefore associated with Cooper pairs and not electrons in the normal state. Second, the induced open circuit voltage yielded the opposite polarity to the input current signal, consistent with the phenomenon of momentum transfer due to CMS [3,9]. Finally, the temperature dependence of the drag current, obtained indirectly from the resistance and open circuit voltage measurements, was consistent with the Coulomb interaction between the normal electrons in the drive wire and the Cooper pairs in the drive wire. However, further experiments are needed to understand why we saw much stronger coupling with our small samples (1 μm wide) than that of our large samples (10 μm wide) and that of Ref. [10] (150 μm wide).

The authors gratefully thank N. Giordano for stimulating discussions that guided us to this approach. The authors also thank W. Porod, C. Lent, S. Ruggiero, G. B. Arnold, J.-M. Duan, Z. Shao, G. Yang, and C. Zhong for very helpful discussions. This work was supported by the Office of Naval Research and the National Science Foundation.

*Electronic address: bernstei@nano2.ee.nd.edu

[1] P. J. Price, Physica (Amsterdam) **117B**, 750 (1983); in *The Physics of Submicron Semiconductor Devices,* edited by H. Grubin, D. K. Ferry, and C. Jacoboni (Plenum, New York, 1988), p. 445.
[2] P. M. Solomon, P. J. Price, D. J. Frank, and D. C. La Tulipe, Phys. Rev. Lett. **63**, 2508 (1989).
[3] T. J. Gramila, J. P. Eisenstein, A. H. MacDonald, L. N. Pfeiffer, and K. W. West, Phys. Rev. Lett. **66**, 1216 (1991); Surf. Sci. **263**, 446 (1992).
[4] P. M. Solomon and B. Laikhtman, Superlattices Microstruct. **10**, 89 (1991).
[5] B. Laikhtman and P. M. Solomon, Phys. Rev. B **41**, 9921 (1990).
[6] H. C. Tso, P. Vasilopoulos, and F. M. Peeters, Phys. Rev. Lett. **68**, 2516 (1992).
[7] H. C. Tso and P. Vasilopoulos, Phys. Rev. B **45**, 1333 (1992).
[8] A. G. Rojo and G. D. Mahan, Phys. Rev. Lett. **68**, 2074 (1992).
[9] J.-M. Duan and S. Yip, Phys. Rev. Lett. **70**, 3647 (1993).
[10] N. Giordano and J. D. Monnier, Phys. Rev. B **50**, 9363 (1994).
[11] Y. M. Wan, S. E. Hebboul, D. C. Harris, and J. C. Garland, Phys. Rev. Lett. **71**, 157 (1993).
[12] G. Deutscher, H. Fenichel, M. Gershenson, E. Grünbaum, and Z. Ovadyahu, J. Low Temp. Phys. **10**, 231 (1973).
[13] G. Bazàn and G. H. Bernstein, J. Vac. Sci. Technol. A **11**, 1745 (1993).
[14] R. E. Simpson, *Introductory Electronics for Sientists and Engineers* (Allyn and Bacon, Boston, 1987), p. 35.
[15] T. P. Orlando and K. A. Delin, *Foundations of Applied Superconductiviy* (Addison-Wesley, New York, 1991), p. 96.